CORROSION INHIBITION BY RARE EARTH CHLORIDES FOR 2219–T87 ALUMINIUM ALLOY IN SEAWATER

Venkatasubramanian G.[1], Sheik Mideen A.[2] and Abhay K Jha[3]

[1,2]Department of Chemistry, Sathyabama University, Jeppiaar Nagar, Chennai, India
[3]Materials Characterisation Division, Vikram Sarabhai Space Centre, Indian Space Research Organization, Thiruvananthapuram, India
Email: [2]smideen@yahoo.co.in

Abstract

The inhibiting effect of cerium chloride and lanthanum chloride on the corrosion of 2219–T87 aluminium alloy (AA2219–T87) in seawater was investigated by potentiodynamic polarisation, electrochemical impedance spectroscopy and scanning electron microscopy coupled with energy dispersive spectroscopy. It is found from potentiodynamic polarisation curves that cerium chloride and lanthanum chloride serve as cathodic inhibitors. The decrease in charge transfer resistance after the addition of rare earth chlorides further confirmed their inhibition on AA2219–T87 towards seawater environment. Scanning electron microscopy and energy dispersive spectroscopy analysis revealed the formation of cerium and lanthanum hydroxide/oxide deposits on second phase intermetallic particles (Al_2Cu) confirmed their cathodic inhibition. Cerium chloride exhibited better inhibition efficiency than lanthanum chloride due to the lower solubility of cerium hydroxide.

Keywords: AA2219-T87; Rare earth inhibitors; Potentiodynamic polarisation; Electrochemical impedance spectroscopy; Scanning electron microscopy.

I. INTRODUCTION

The reusable solid rocket boosters (SRB) made with AA2219 aluminium alloy (AA2219) is used to transport the space shuttle to low earth orbit. After fuel exhaustion, the booster detaches from the launch vehicle, parachutes into the ocean, and is retrieved within 36 hours. During this period, severe corrosion damage was observed in SRB due to the presence of aggressive chloride ions in seawater [Danford *et al.* 1995].

A number of older works have been published on the seawater corrosion resistance of aluminium alloys [Godard *et al.* 1965, 1967; Speidel *et al.* 1976; Bozack *et al.* 1993]. Recently the corrosion behaviour of difference zones of AA2219-T87 gas tungsten arc welded plate in sea water has been reported [Venkatasubramanian *et al.* 2012] and results showed that heat affected zone is more prone to corrosion than weld zone and base metal. The high-strength aircraft alloys (Al–Cu and Al–Zn–Mg–Cu) are considered to have poor corrosion resistance to seawater, and in the unprotected state a 0.25 inch plate has been observed to perforate in a few years. Generally a high passivity protective oxide layer is formed with greater thickness on the surface of aluminium alloys in aqueous environment [Schumacher, 1979]. However, the presence of chloride ions in an aggressive solution like seawater breaks the oxide layer [Dabala *et al.* 2004] and leads to the formation of galvanic couples and micro-flaws for pit nucleation and growth [Wang *et al.* 2012].

Chemical conversion coating is an important and commonly adopted technique to prevent the corrosion particularly in structural aluminium alloys. This type of coating by chromate processes is helpful in improving the paint adhesion and also corrosion inhibition [Kendig *et al.* 2001; Zhao et al. 2001; Lunder *et al.* 2005]. Due to the strong oxidizing power of chromates, it inhibits the corrosion by forming a passive layer on the aluminium alloy surface [Kendig, 1993]. Due to high toxicity of hexavalent chromium and subsequent environmental hazards [Bahadur, 1992; Kendig *et al.* 2001], researchers intensely tried an alternate as inhibitors to replace the chromates. The rare earth metals have been identified by researchers as a green substitute for the chromate species not only because of their effectiveness but also due to their null toxicity [Hinton *et al.* 1984; Bethencourt *et al.* 1998]. Recently, the rare earth salts have been reported as potential inhibitors for AA2014 [Mishra *et al.* 2007], AA2024 [Kiryl A. Yasakau *et al.* 2006] and AA2024–T3 [Muster *et al.* 2007; Rosero-Navarro *et al.* 2010] in 3.5% NaCl solution. In aluminium-copper alloys, the cathodic sites are blocked by cerium or lanthanum as its oxide or

hydroxide and act as cathodic inhibitor by reducing the cathodic current.

Characterisation of the surface damage caused by seawater and the inhibitive effects of rare earth metal deposits on AA2219–T87 provides the motivation for the present investigation and the major objective is to evaluate the inhibition efficiency of cerium chloride and lanthanum chloride on the corrosion of AA2219–T87 in seawater and to elucidate their inhibition mechanism.

II. EXPERIMENTAL

A. Materials preparation

A 7.4 mm thick AA2219 aluminium alloy plate with a nominal chemical composition 5.95Cu – 0.27Mn – 0.12Zr – 0.09V – 0.06Ti– 0.12Fe – 0.05Si (wt. %) was used in the present investigation. The alloy was received in the T87 temper condition (solutionized at 535°C for 45 minutes followed by 7% cold rolling and a subsequent aging treatment at 165°C for 24 hours) to obtain a stabilised microstructure. The major second phase intermetallic particles present in this alloy is θ phase with a chemical composition Al_2Cu.

The working electrodes (WE) used for potentiodynamic polarisation and electrochemical impedance spectroscopy (EIS) tests were prepared by using the following procedure. The AA2219–T87 plate was cut in transverse direction parallel to the rolling direction. Then the WE was soldered with Cu-wire for electrical connection and was embedded in epoxy resin to expose a geometrical surface area of 1 cm^2 to the electrolyte. The electrodes were mechanically abraded with 800, 1000, 1200 grade silicon carbide sheets. Then these were polished to mirror smooth by 1 μm finish using rotating disc with non-aqueous diamond paste, degreased by acetone, washed with double distilled water and dried. For microstructural examinations, the samples were sectioned and polished down to 5 μm alumina finish followed by etching in Keller's reagent [2.5ml HNO_3 (60%) + 1.5ml HCl (37%) + 1ml HF (48%) + 95 ml of double distilled water]).

B. Testing solutions

The seawater was obtained from the ocean surface near East Costal Area, Chennai, India and its pH (8.23) was measured with a digital pH meter calibrated against standard solutions. Analytical grade reagents of $CeCl_3$ and $LaCl_3$ were used as inhibitors without further purification in the concentration range from 250 to 1000 ppm(mg./lit.). For each experiment, a freshly prepared solution was used. During the experiments, the test solutions were opened to air. The temperature of solution was thermostatically controlled at 30°C.

C. Techniques

The polarisation and impedance measurements experiments were conducted with software based Bio-analytical system [BAS-Zahner, make IM6–electrochemical analyzer model using Thales software]. Potentiodynamic polarisation curves were obtained with a scan rate of 0.5 mV sec^{-1} in the potential range from -250 to $+250$ mV relative to the open circuit potential. Corrosion current density values were obtained by Tafel extrapolation method. The EIS measurements were carried out using a potentiostat(same instrument which was used in the previous potentiodynamic polarisation experiment) coupled to a frequency response analyzer system in the frequency range of 100 kHz to 100 mHz with amplitude of 10 mV peak to peak using AC signals at open circuit potential. The cell was equipped with a flat plate of AA2219–T87 as the working electrode, a saturated calomel electrode (SCE) as the reference electrode, and a graphite electrode as the counter electrode. Potentiodynamic polarisation and EIS measurements were performed after initial delay of 10 minutes for the sample to reach a steady state condition.

For microstructural examinations, full immersion tests for AA2219-T87 samples in seawater with and without inhibitors were performed for 24 hours at room temperature in accordance with ASTM-G31 standard. The corrosion products were removed as per ASTM-G1 standard. The surface morphology of the samples were analysed by optical microscopy (Inverted Metallurgical Microscope, G'71 OLYMPUS, Japan) and scanning electron microscopy (SEM) coupled with energy dispersive spectroscopy (EDX) (FESEM-SUPRA55, CARL ZEISS, Germany).

III. RESULTS AND DISCUSSION

A. Potentiodynamic polarisation

The potentiodynamic polarisation curves of AA2219–T87 in seawater in the absence and presence of various concentrations of $CeCl_3$ and $LaCl_3$ are shown in Fig. 1 and Fig. 2 respectively. As it can be seen from figures that the cathodic reactions are inhibited after the addition of $CeCl_3$ and $LaCl_3$ to the aggressive solution, and this inhibition more and more pronounces with increasing inhibitor concentration. Corrosion potential (E_{corr}) of AA2219–T87 was shifted to more negative potential in the presence of inhibitors when compared to that observed in seawater (from –569 mV to –737 mV for $CeCl_3$ addition and –618 mV for $LaCl_3$ addition). The cathodic inhibition of cerium and lanthanum salts are further supported by the increase in cathodic slope from –337 mV/dec (AA2219–T87 in sea water) to –27 mV/dec (with 1000 ppm $CeCl_3$) and –83 mV/dec (with 1000 ppm $Lacl_3$). Hinton [1989] relates the concentrations of rare earths and their inhibiting efficiency with two factors: the pH of the solution and the nature of the protective layer, which depends both on the type of cation and its concentration. According to Aramaki [2011], cerium and lanthanum oxide not only precipitates on intermetallics at the expense of the oxygen reduction, but the reduction of H^+ plays a fundamental role in the precipitation. It can be observed from Tafel polarisation curves that the corrosion current densities were decreased from 1.24 μ A/cm^2 to 0.0164 μ A/cm^2 upon the addition of cerium chloride and to 0.124 μ A/cm^2 for the addition of Lanthanum chloride gradually from 250 ppm to 1000 ppm. Little passivation was observed in the anodic portion of the curves in both the cases which may be due to the pH of seawater around ≈ 8.23.

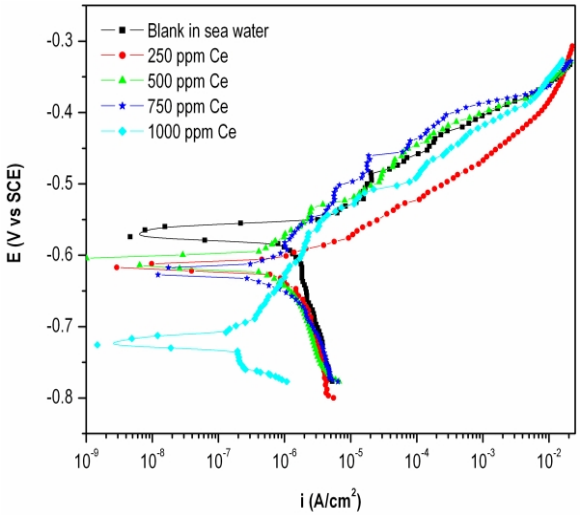

Fig. 1. Potentiodynamic polarisation curves of AA2219-T87 aluminium alloy in seawater in the presence and absence of various concentrations of $CeCl_3$

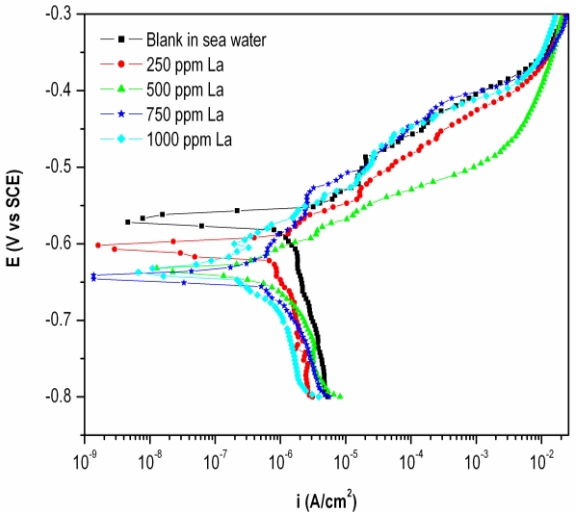

Fig. 2. Potentiodynamic polarisation curves of AA2219-T87 aluminium alloy in seawater in the presence and absence of various concentrations of $LaCl_3$

The electrochemical parameters of AA2219–T87 in seawater with and without inhibitor addition were determined from polarisation measurements and are shown in Table 1. The inhibition efficiency (I.E %) was calculated from polarisation measurements according to following equation:

$$I.E\,(\%) = \left[\frac{i^{\circ}_{corr} - i_{corr}}{i^{\circ}_{corr}} \right] \times 100$$

where, and i°_{corr} are corrosion current densities in the absence and presence of inhibitor respectively. The decrease in i_{corr} values confirmed the increase in percentage of inhibition efficiency with inhibitor concentration. Fig. 3 shows the inhibition values of the inhibitors for corrosion of AA2219-T87 in seawater.

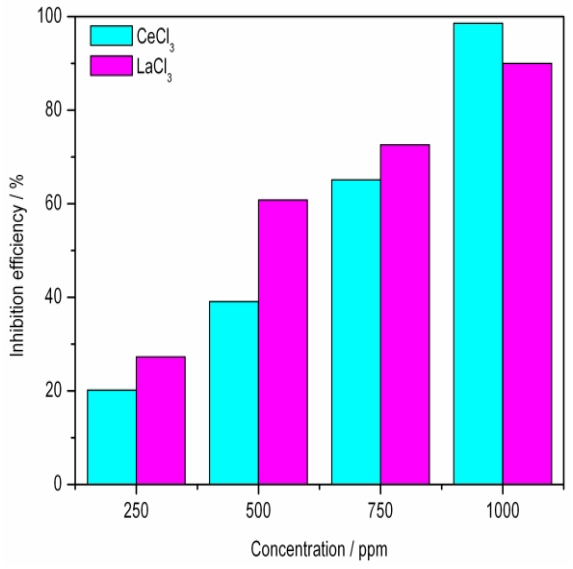

Fig. 3. Inhibition efficiencies of various concentrations of $CeCl_3$ and $LaCl_3$ in seawater on AA2219-T87 aluminium alloy using i_{corr}

B. Electrochemical impedance spectroscopy

The Nyquist plots of AA2219-T87 obtained in seawater with and without the presence of various concentrations of $CeCl_3$ and $LaCl_3$ are shown in Fig. 4 and Fig. 5 respectively. As it can be seen from these figures that the Nyquist plots contain one depressed semicircle followed by loop, indicates the corrosion of AA2219-T87 is mainly controlled by a charge transfer process. The depressed semicircles are the characteristic of the solid electrodes and generally referred to as frequency dispersion, which has been attributed to roughness and inhomogeneities of the solid surfaces caused by hard Al_2Cu intermetallic particles on aluminium alloy surfaces. The diameter of semicircle corresponding to charge transfer resistance indicates the corrosion rate. The inhibition efficiency was calculated from charge transfer resistance measurements according to following equation:

$$I.E\,(\%) = \left[\frac{R_{ct} - \overset{\circ}{R_{ct}}}{R_{ct}}\right] \times 100$$

where, R_{ct} is the charge transfer resistance of inhibited solution and is charge transfer resistance of uninhibited solution. The uninhibited sample showed a low charge transfer resistance (R_{ct} = 5.69 kÙ cm^2) in sea water. The increase of R_{ct} values of 18.79 k Ω cm^2 for 1000 ppm of $CeCl_3$ and 17.31 kΩ cm^2 for 1000 ppm of $LaCl_3$ supports inhibition action of these rare earth chlorides. Fig. 6 shows the inhibition values of the inhibitors based on R_{ct}values for corrosion of AA2219-T87 in sea water. The inhibition efficiency value increases with concentration up to 1000 ppm, indicating the maximum 69.7% for $CeCl_3$ and 67.1% for $LaCl_3$. The high-frequency semicircle existing in the Nyquist plot is associated with the formation cerium and lanthanum oxide/hydroxide deposits. Furthermore, these deposits are sufficiently thick to cover the second phase particles, eliminating the galvanic coupling effect between the second phase

Table 1. Corrosion parameters obtained from Tafel polarisation curves for AA2219-T87 aluminium alloy in sea water with and without $CeCl_3$ and $LaCl_3$ inhibitors

Solution	Parameters									
	E_{corr} vs SCE (mV)		I_{corr} (μ A/cm^2)		βc (mV/dec)		βa (mV/dec)		Inhibition efficiency (%)	
	$CeCl_3$	$LaCl_3$	$CeCl_3$	$LaCl_3$	$CeCl_3$	$LaCl_3$	$CeCl_3$	$LaCl_3$	$CeCl_3$	$LaCl_3$
Blank	– 569	– 569	1.24	1.24	– 337	– 337	43.4	43.4		
250 ppm	– 600	– 586	0.99	0.901	– 245	– 403	26	42	20.1	27.3
500 ppm	– 581	– 616	0.755	0.485	– 253	– 129	61	36	39.1	60.8
750 ppm	– 611	– 636	0.433	0.339	– 99	– 93	48	110	65.1	72.6
1000 ppm	– 737	– 618	0.016	0.124	– 27	– 83	32	55	98.6	90

particles and aluminium alloy substrate. Consequently, the corrosion of aluminium alloy is inhibited remarkably. The Impedance parameters of AA2219–T87 in seawater with and without inhibitor addition were determined from Nyquist plot and are given in Table 2

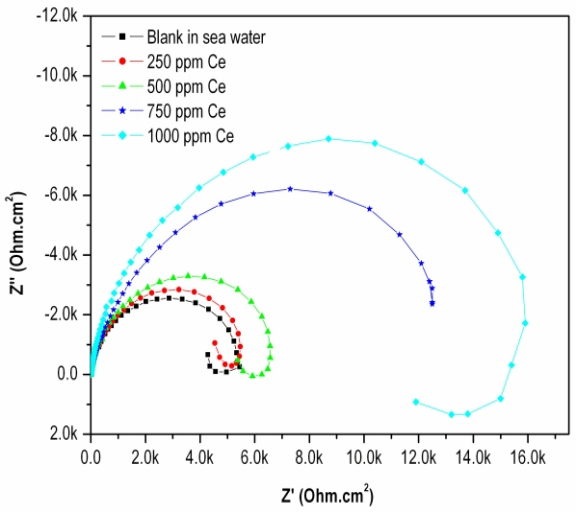

Fig. 4. Nyquist spectra of AA2219-T87 aluminium alloy in seawater containing different concentrations of $CeCl_3$

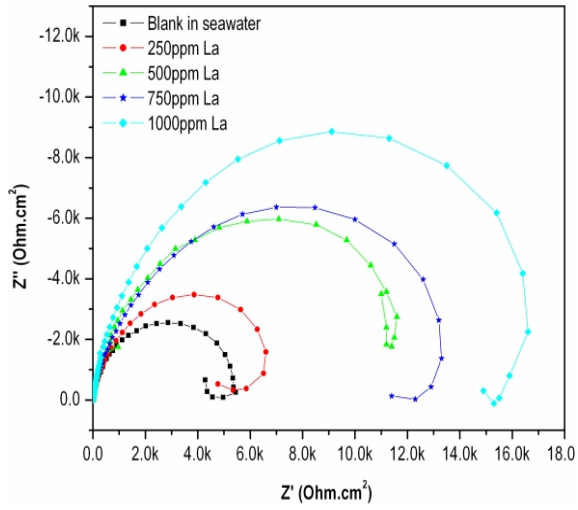

Fig. 5. Nyquist spectra of AA2219-T87 aluminium alloy in seawater containing different concentrations of $LaCl_3$

The capacitance connected in parallel to the charge transfer resistance corresponds to interfacial capacitance, C_{dl} and therefore may approximately indicate the expanded surface area of the corroding

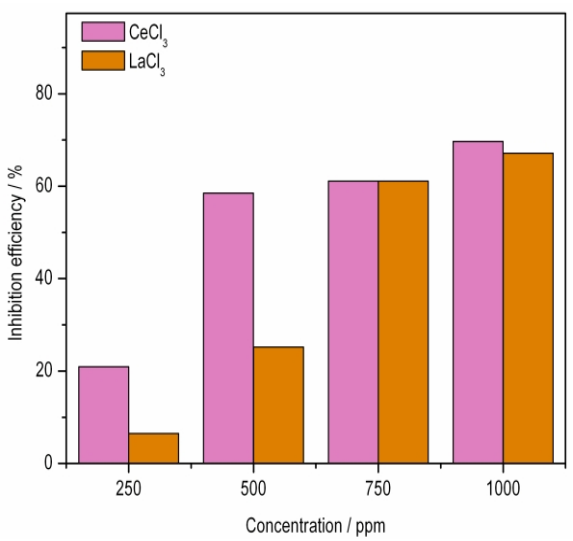

Fig. 6. Inhibition efficiencies of various concentrations of $CeCl_3$ and $LaCl_3$ in seawater on AA2219-T87 aluminium alloy using R_{ct}

electrode. This was calculated using the following formula:

$$C_{dl} = \left(\frac{1}{2 \pi f_{max}} \right) \times \left(\frac{1}{R_{ct}} \right)$$

where, f_{max} is the maximum frequency obtained from the Nyquist plots. The double layer capacitance (C_{dl}) is inversely proportional to thickness of the film. So a decrease in C_{dl} by increasing concentration implies the increase in thickness of the film(cerium or lanthanum oxide/hydroxide) in both the cases. The C_{dl} of AA2219–T87 in uninhibited sea water showed 4.3 μ F/cm^2, but there is an appreciable decrease in the value as 2.06 μ F/cm^2 and 2.69 μ F/cm^2 in presence of 1000ppm of $CeCl_3$ and 1000ppm of $LaCl_3$ respectively. This decrease in C_{dl} is due to the formation of reaction products, lanthanum or cerium oxide/hydroxide on the cathodic intermetallic particles. Fig. 7 and Fig. 8 demonstrate the Bode impedance plots of AA2219–T87 samples after immersion in sea water and in presence of $CeCl_3$ and $LaCl_3$ solutions. The low-frequency impedance of the corroded metallic electrode can be used as a measure of the corrosion activity. As it can be shown in Fig. 7 and Fig. 8 that AA2219–T87 immersed in the inhibitor free sea water has the minimal value of the low-frequency impedance (4.35 k Ω cm^2). However, the presence of chlorides of cerium and lanthanum with 1000 ppm concentration in

Table 2. Impedance parameters extracted from Nyquist plots for AA2219-T87 aluminium alloy in seawater with and without $CeCl_3$ and $LaCl_3$ inhibitors

Solution	Parameters					
	R_{ct} ($k\Omega\ cm^2$)		C_{dl} (μ F cm^{-2})		Inhibition efficiency (%)	
	$CeCl_3$	$LaCl_3$	$CeCl_3$	$LaCl_3$	$CeCl_3$	$LaCl_3$
Blank	5.69	5.69	4.3	4.3		
250 ppm	7.199	6.088	3.34	4.519	20.9	6.5
500 ppm	13.713	7.614	3.386	8.094	58.5	25.2
750 ppm	14.629	14.626	5.276	4.476	61.1	61.1
1000 ppm	18.791	17.312	2.69	2.066	69.7	67.1

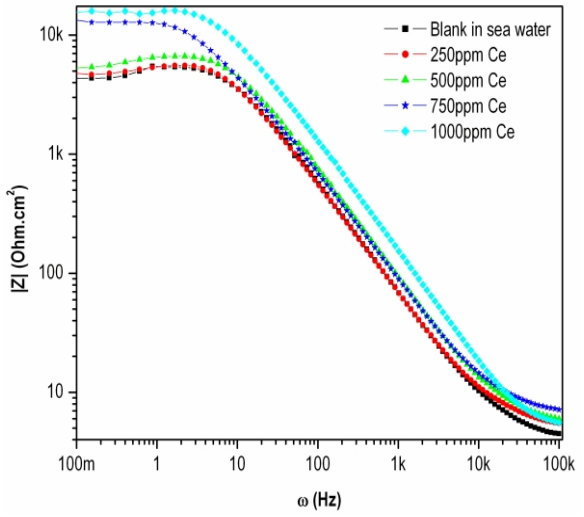

Fig. 7. Bode plot for AA2219-T87 aluminium alloy in seawater containing various concentrations $CeCl_3$

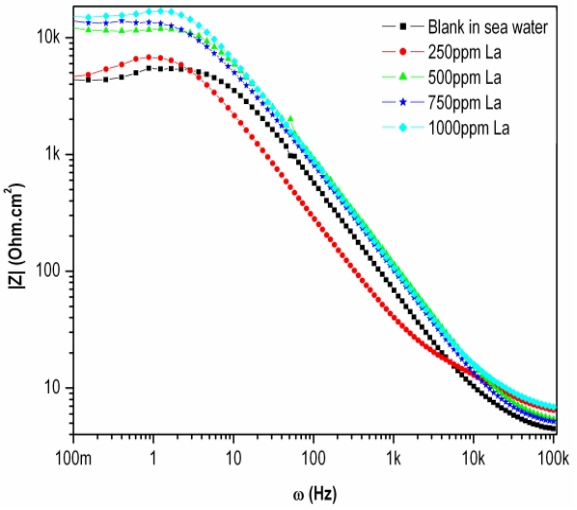

Fig. 8. Bode plot for AA2219-T87 aluminium alloy in seawater containing various concentrations $LaCl_3$

seawater increased the low frequency impedance values, 15.4 k Ω cm^2 and 15.2 k Ωcm^2 respectively. These results revealed the inhibiting action of rare earth chlorides on AA2219–T87 and conferring their protective efficiency against seawater corrosion. This is also in well agreement with the Tafel plot results.

C. Microstructure, SEM and EDX analyses

Scanning electron microscopy (SEM) and energy dispersive spectroscopy (EDX) techniques were employed in order to get additional information on the inhibition mechanism. Optical microstructure of the parent metal (Fig. 9) revealed elongated grains in the rolling direction with the precipitates of Al_2Cu particles along the grain boundaries as well as within the grains, which is typical microstructure of AA2219, rolled plate in T87 temper condition [Venugopal et al. 2012]. Subsequent examination under a scanning electron microscopy demonstrates that the segregated copper-rich phases appeared as a white network (Fig. 10a). Elemental analysis of the particles in this regions (Fig. 10b) revealed Cu/Al a weight ratio of 39.87/60 corresponds to $\theta-$ phase particles.

The SEM images of AA2219–T87 after an exposure period of 24 hours in seawater were represented in Fig. 11a and 11b. It can be noted that a severe localised corrosion in the form of pits was observed in the BM, preferentially the areas adjacent to Al_2Cu particles as they were cathodic phases when

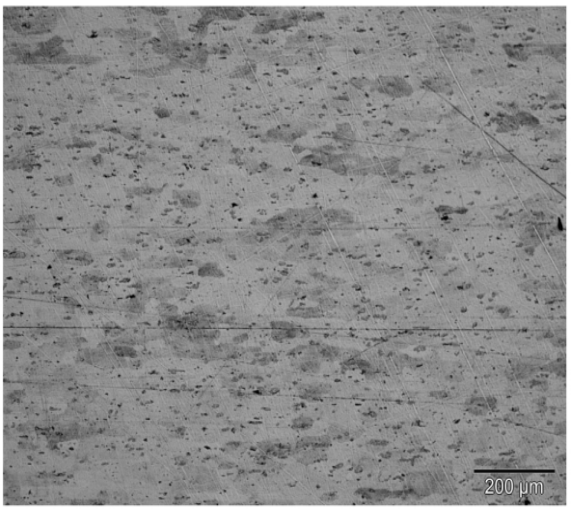

Fig. 9. Optical micrograph of AA2219-T87 aluminium alloy polished surface

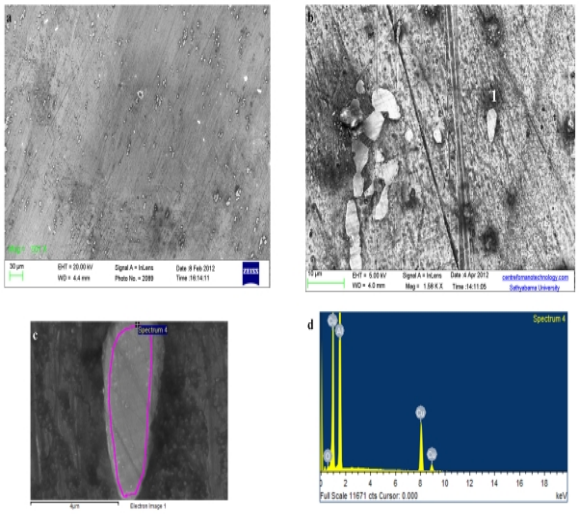

Fig. 10. SEM image of AA2219-T87 aluminium alloy surface, (a) Lower magnification, (b) Higher magnification, (c) Enlarged version of particle 1(Al_2Cu) from fig. b, (d) EDX spectra of Al_2Cu

compared with the matrix aluminium. The EDX spectra of the corroded regions of pit 1 (Fig. 11c) revealed dissolution of θ – phase particles which showed a lower Cu/Al weight ratio of 22.06/65.65. Presence of calcium and sulphur was also observed in EDX analysis because of the seawater. The deep pits formed on the surfaces due to the dissolution of second

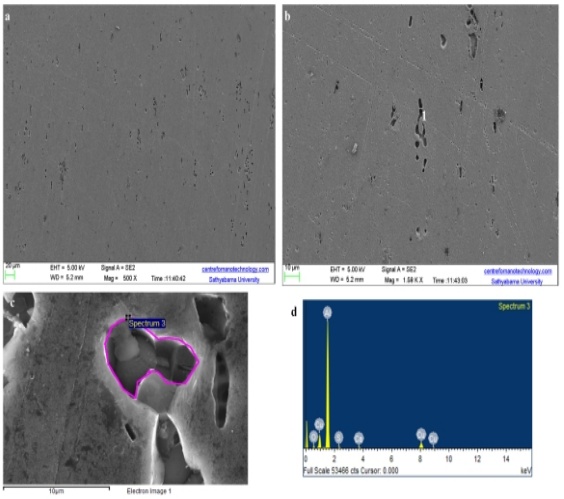

Fig. 11. SEM image of AA2219-T87 aluminium alloy surface immersed in sea water for 24 hrs. (a) Lower magnification, (b) Higher magnification, (c) Enlarged version of pit 1 from fig. b, (d) EDX spectra of pit 1

phase Al_2Cu intermetallic particles, which act as preferential cathodes causing galvanic coupling and preferential dissolution of the aluminium matrix surrounding them. This result is in well agreement with Mazurkiewicz *et al* [1983].

Typical SEM images with EDX spectra of AA2219–T87 specimens exposed to seawater with 1000 ppm of $CeCl_3$ and 1000 ppm of $LaCl_3$ for 24 hours are shown in Fig. 12a–12d and Fig. 13a–13d respectively. The clearly visible polishing marks on the surfaces and lesser number of pits indicate the absence of intermetallic de-alloying in the presence of inhibitors. The discrete small shape deposits of cerium/lanthanum oxides and/or hydroxides were observed on the alloy surfaces particularly, the cerium and lanthanum rich particles were found and they were associated only with second phase θ – particles. The EDX spectra of the inhibited samples marked as particle 1 in Fig. 12c and Fig. 13c respectively further revealed the presence of cerium and lanthanum atoms along with Cu/Al ratio of Al_2Cu particles confirmed cathodic nature of inhibitors and overall decrease in the corrosion rate of AA2219–T87 in seawater.

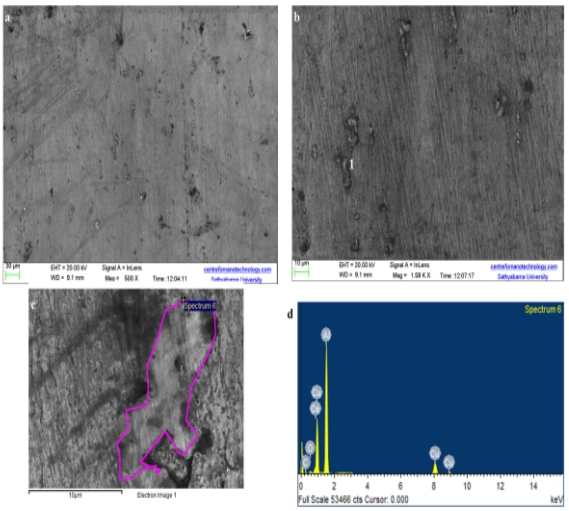

Fig. 12. SEM image of AA2219-T87 aluminium alloy surface immersed in sea water with 1000 ppm of $CeCl_3$ for 24 hrs. (a) Lower magnification, (b) Higher magnification, (c) Enlarged version of particle 1 from fig. b, (d) EDX spectra of particle 1

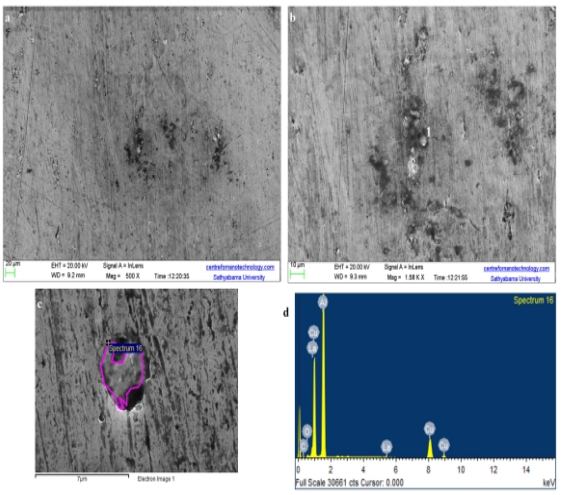

Fig. 13. SEM image of AA2219-T87 aluminium alloy surface immersed in sea water with 1000 ppm of $LaCl_3$ for 24 hrs. (a) Lower magnification, (b) Higher magnification, (c) Enlarged version of particle 1 in fig. b, (d) EDX spectra of particle 1

D. Mechanism of inhibition

It has been reported that the oxygen reduction reaction is more favoured on Cu-rich intermetallic particles in chloride containing aqueous solutions [Mazurkiewicz *et al.* 1983; Buchheit, 1995]. The cathodic reaction (Equation 1) occurring at the cathodic sites are dominated by the reduction of oxygen in turn increases local pH by generating a high concentration of OH^- ions and promotes dissolution of the aluminium matrix near and adjacent to the cathodic intermetallic particles, causing severe localized attack [Dimitrov *et al.* 1999, 2001; Buchheit *et al.* 1997; Ilevbare *et al.* 2001].

$$O_2 + 2H_2O + 4e \rightarrow 4OH \qquad ...(1)$$

These OH^- ions formed over the cathodic sites are expected to react with the lanthanide ions (Ce^{3+} or La^{3+} ions) present in the solution. The reactions give rise to the precipitation of lanthanide oxides or hydroxides over cathodic sites and the nodule formation (Equations: 2, 3).

$$Ce^{3+} + 3OH \rightarrow Ce(OH)_3 \qquad ...(2)$$

$$La^{3+} + 3OH \rightarrow La(OH)_3 \qquad ...(3)$$

Blocking of the cathodic sites by these nodules decreases the available cathodic current and, therefore, reduces the principal corrosion process of AA2219–T87 alloy, the alkaline localised pitting. This explanation is supported by the results of several authors [Mansfeld *et al.* 1991, 1994; Aldekiewicz *et al.* 1995]. According to the Pourbaix diagram the compound of cerium was more stable than compound of lanthanum in the neutral or slightly acidic solution [Pourbaix, 1966] and suggested that the inhibiting ability of Ce^{3+} ion is better than that of La^{3+} ion.

IV. CONCLUSIONS

From the results obtained, the following points can be concluded:

1. Both cerium chloride and lanthanum chloride show good inhibition efficiency for the corrosion of AA2219–T87 aluminium alloy in seawater. Their inhibition efficiency increases with inhibitor concentration.

2. The potentiodynamic polarization curves indicate that cerium chloride and lanthanum chloride serve as cathodic inhibitors for AA2219–T87 aluminium alloy in seawater by controlling the rate of oxygen reduction reactions. Their inhibition efficiency is

further confirmed by electrochemical impedance spectroscopy.

3. Scanning electron microscopy and energy dispersive spectroscopy analysis revealed the formation of cerium and lanthanum hydroxide/oxide deposits on second phase intermetallic particles (Al_2Cu), which decreases the available cathodic current and, therefore, reduces the localised pitting corrosion of AA2219–T87 aluminium alloy in seawater.

4. Cerium chloride exhibited better inhibition efficiency than lanthanum chloride due to the lower solubility of cerium hydroxide.

ACKNOWLEDGEMENTS

The authors would like to thank Vikram Sarabhai Space Centre, Indian Space Research Organisation, Thiruvananthapuram for financial support (Project Number: 10/3/508, dated 9th March 2004).

REFERENCES

[1] Aldekiewicz. A. J, Isaacs. H. S, Davenport. A. J, 1995, The Investigation of Cerium as a Cathodic Inhibitor for Aluminum-Copper Alloys, Journal of Electrochemical Society, Vol. 142, pp. 3342-3350

[2] Aramaki. K, 2001, The inhibition effects of cation inhibitors on corrosion of zinc in aerated 0.5 M NaCl, Corrosion Science, Vol. 43, pp. 1573–1588

[3] Bahadur A, 1992, Chromates as corrosion inhibitors for aqueous systems, Corrosion Review, Vol. 10, pp.155

[4] Bethencourt. M, .Botana. F. J, Calvino. J. J, Marco. M and Rodriguez-Chacon.M. A, 1998, Lanthanide compounds as environmentally friendly corrosion inhibitors of aluminium alloys: A Review, Corrosion Science, Vol. 40(11), pp.1803-1819

[5] Bozack. M. J. and Beshears. R. D, 1993, The effects of exposure temperature on 2219 Al-Cu alloy surfaces immersed in natural seawater, Corrosion Science, Vol. 34 (4), pp. 631–653

[6] Buchheit. R.G, 1995, A compilation of corrosion potentials reported for intermetallic phases in aluminium alloys, Journal of Electrochemical Society Vol. 142, pp. 3994-3996

[7] Buchheit R. G, Grant R. P, Hlava P. F, McKenzie B, Zender G. L, 1997, Local dissolution phenomena associated with S phase (Al_2CuMg) particles in aluminium alloy 2024-T3, Journal of Electrochemical Society, Vol. 144, pp. 2621-2628

[8] Dabala. M, Ramous. E, Margini. M, 2004, Materials and corrosion, Vol. 55, pp. 381-386

[9] Danford M.D and Mendrek. M.J, February 1995, The corrosion protection of AA2219-T87 by aluminium by organic and inorganic zinc rich primers, NASA Technical Paper 3534, National Aeronautics and Space Administration Marshall Space Flight Center, MSFC, Alabama 35812

[10] Dimitrov N, Mann JA, Vukmirovic M, Sieradzki K, 2000, De-alloying of Al_2CuMg in alkaline media, Journal of Electrochemical Society, Vol. 147, pp. 3283-3285

[11] Dimitrov N, Mann JA, Sieradzki K, 1999, Copper redistribution during corrosion of aluminium alloys, Journal of Electrochemical Society, Vol. 146, pp. 98-102

[12] Godard H.P. and Booth F.F, 1965, Congress International de la Corrosion Marine et des Salissures, Editions du Centre de Recherches et l'Etudes Oceaniques, 1 Quai Branly, Paris 7

[13] Godard H.P, Jepson.W.B, Bothwell. M. R and Robert L. Kane, 1967, The Corrosion of Light Metals, Chapter 1, Wiley, New York

[14] Hinton BRW, Arnott DR, Ryan NE, 1984, The inhibition of aluminium alloy corrosion by cerous cations, Materials Forum, Vol. 7, pp. 211-217

[15] Hinton BRW, Hughes A, Taylor R, Henderson K, Nelson K, Wilson L, 1997, The corrosion protection properties of a cerium oxide conversion coating on aluminium alloy AA2024, ATB Metall Vol. 37, pp.165-168

[16] Hinton BRW, Raman A, Labine P (Eds.) 1989, Review on Corrosion Inhibitor Science and Technology, Corrosion/1989 Symposium, NACE, Paper No. I-11, 1-19

[17] Ilevbare GO, Scully JR, 2001, Mass transport-limited oxygen reduction reaction on AA2024-T3 and selected intermetallic compounds in chromate-containing solutions, Corrosion, Vol. 57, pp.134.

[18] Kendig. M, Jeanjaquet . S, Addison. R, Waldrop. J, 2001, Role of hexavalent chromium in the inhibition of corrosion of aluminium alloys, Surface Coating and Technology, Vol. 140, pp. 58–66.

[19] Kendig M, Davenport AJ, Isaacs HS, 1993, The mechanism of corrosion inhibition by chromate conversion coatings from x-ray absorption near edge spectroscopy (Xanes), Corrosion Science, Vol. 34, pp.4

[20] Kiryl A. Yasakau, Mikhail L. Zheludkevich, Sviatlana V. Lamaka, Mario G. S. Ferreira, 2006, Mechanism of corrosion inhibition of AA2024 by rare-earth compounds, Journal of Physical Chemistry B, Vol. 110 (11), pp. 5515–5528

[21] Lunder. O, Walmsley. J. C, Mack. P, Nisancioglu. K, 2005, Formation and characterisation of a chromate conversion coating on AA6060 aluminium, Corrosion Science, Vol. 47, pp.1604–1624

[22] Mansfeld. F, Wang. Y, 1994, Corrosion protection of high copper aluminium alloys by surface modification, British Corrosion Journal, Vol. 29, pp.194-200

[23] Mansfeld. F, Wang. Y, Shih. H, 1991, Development of stainless aluminium, Journal of Electrochemical Society. Vol. 138, pp.L74-L75

[24] Mazurkiewicz B, Piotrowski A, 1983, The electrochemical behaviour of the Al_2Cu intermetallic compound, Corrosion Science, Vol. 23, pp. 697-707

[25] Mishra AK, Blasubramanian R, 2007, Corrosion inhibition of aluminum alloy AA 2014 by rare earth chlorides, Corrosion Science, Vol. 49, pp.1027–1044

[26] Muster. T. H, Lau. D, Wrubel. H, Sherman . N, Hughes. A. E, Harvey. T. G, Markley . T, Alexander. D. L. J, Corrigan. P. A, White.P.A, Hardin. S. G., Glenn. M. A, Mardel. J, Garcia.S. J, Mol. J. M. C, 2010, An investigation of rare earth chloride mixtures: combinatorial optimisation for AA2024-T3 corrosion inhibition, Surface and Interface Analysis, Vol. 42(4), pp.170–174

[27] Pourbaix M, 1966, Atlas of electrochemical equilibria in aqueous solutions, Pergamon Press, London, p183

[28] Rosero-Navarro. N. C, Curioni. M, Bingham. R, Durán. A, Aparicio. M, Cottis. R. A, and Thom. G. E, 2010, Electrochemical techniques for practical evaluation of corrosion inhibitor effectiveness: Performance of cerium nitrate as corrosion inhibitor for AA2024-T3 alloy, Corrosion Science, Vol. 52, pp.3356-3366

[29] Schumacher. M, 1979, Seawater corrosion handbook, William Andrew Publishing/Noyes

[30] Speidel. M. O. and Hyatt. M. V, 1976, Advances in Corrosion Science and Technology, Vol. 2 (eds M. G. Fontana and R. W. Staehle), Chapter 3, Plenum Press, New York

[31] Venkatasubramanian. G, Sheik Mideen. A, Abhay Jha. K, 2012, Corrosion behaviour of aluminium alloy AA219-T87 welded plates in seawater, Indian Journal of Science and Technology, Vol. 5(11), pp. 3578-3583

[32] Venugopal. A, Sreekumar. K, and Raja V.S, March 2012, Stress corrosion cracking behaviour of multipass TIG-welded AA2219 aluminium alloy in 3.5 wt pct NaCl solution, Metallurgical and Materials Transactions A, DOI: 10.1007/s11661-012-1117-5

[33] Wang.B.B, WangY.Z, Han.W, Ke.W, 2012, Atmospheric corrosion of aluminium alloy 2024-T3 exposed to salt lake environment in Western China, Corros.ion Science, Vol. 59, pp.63-70

[34] Zhao. J, Xia. L, Sehgal. I. A, Lu. D, McCreery. R. L, G.S. Frankel. G. S, 2001, Effects of chromate and chromate conversion coatings on corrosion of aluminium alloy 2024-T3, Surface Coatings and Technology, Vol. 140, pp.51–57

Mr. G. Venkatasubramanian is a research scholar of Sathyabama University in the department of chemistry. He has more than 15 years of academic and 9 years of industrial experience. He is currently doing research in the corrosion behaviour of aluminium alloys used for space applications. He has seven publications both in reputed journals and conferences to his credit.